

Stefano Iubini · Antonio Politi ·
Paolo Politi

Coarsening dynamics in a simplified DNLS model

Received: date / Accepted: date

Abstract We investigate the coarsening evolution occurring in a simplified stochastic model of the Discrete NonLinear Schrödinger (DNLS) equation in the so-called negative-temperature region. We provide an explanation of the coarsening exponent $n = 1/3$, by invoking an analogy with a suitable exclusion process. In spite of the equivalence with the exponent observed in other known universality classes, this model is certainly different, in that it refers to a dynamics with two conservation laws.

Keywords Coarsening · Exclusion processes · Breathers

1 Introduction

The DNLS model [1] (with a positive defined quartic term) is known to be characterized by a so-called negative temperature region, where localized solutions (breathers) spontaneously arise and survive for long times [2,3]. In a series of theoretical papers, Rumpf [4,5,6,7] has shown, with the help of entropic arguments, that the system is expected to converge towards a state

Stefano Iubini
Dipartimento di Fisica e Astronomia - CSDC, Università di Firenze, via G. Sansone
1 I-50019, Sesto Fiorentino, Italy
E-mail: stefano.iubini@fi.isc.cnr.it

Antonio Politi
Institute for Complex Systems and Mathematical Biology & SUPA University of
Aberdeen, Aberdeen AB24 3UE, United Kingdom
E-mail: a.politi@abdn.ac.uk

Paolo Politi · Stefano Iubini
Istituto dei Sistemi Complessi, Consiglio Nazionale delle Ricerche, via Madonna
del Piano 10, I-50019 Sesto Fiorentino, Italy
INFN Sezione di Firenze, via G. Sansone 1 I-50019, Sesto Fiorentino, Italy
E-mail: Paolo.Politi@isc.cnr.it

characterized by a single breather sitting on a homogeneous background at infinite temperature. Nevertheless, a detailed numerical study [8] has recently challenged such a conclusion, since the process turns out to be both extremely slow and accompanied by the continuous birth and death of breathers.

A clarification of the asymptotic regime in the original DNLS model is a rather ambitious task, because of both its nonlinear character and the weak coupling between breathers and background. In order to overcome such difficulties, a purely stochastic Microcanonical Monte Carlo (MMC) model was proposed in Ref. [8] with the goal of exploring the role of entropy not only in the identification of the asymptotic state, but also for the characterization of the convergence process. Analogously to the DNLS equation, the MMC model is characterized by two conservation laws (energy and norm) and by a local evolution rule. More precisely, such constraints are representative of the original DNLS dynamics in the high-norm density limit, where the interaction energy between neighbouring sites is negligible. In Ref. [8] it was discovered that the MMC dynamics is characterized by a coarsening process during which the localized solutions progressively disappear, while their typical height increases. On the one hand, the purely stochastic character of the MMC model makes it doubtful that the resulting evolution is able to reproduce the key features of the DNLS dynamics. On the other hand, its study can help to clarify the kind of constraints that are expected to emerge during the convergence to the asymptotic state.

Coarsening is a fairly common feature of out-of-equilibrium systems, either relaxing towards equilibrium [9] or kept well far from equilibrium [10]. It corresponds to a growth of the typical length scale L of the system, which usually increases with a power law, $L(t) \approx t^n$, which defines the coarsening exponent n . According to the value of n , different universality classes can be defined, which depend, first of all, on conservation laws. Two exponents, $n = 1/2$ and $n = 1/3$, are specially widespread. They correspond to diffusive processes with ($n = 1/3$) and without ($n = 1/2$) the conservation of the order parameter. The simplest models displaying such coarsening behaviour are the so-called models A and B of dynamics [11], which represent, for example, the relaxation to equilibrium of a deeply quenched Ising model, when the magnetization is not conserved (model A) or is conserved (model B) by dynamics. The latter case, because of the equivalence between Ising and lattice gas model, makes the exponent $n = 1/3$ of special relevance for condensation processes and for large classes of nonequilibrium statistical mechanics models [12].

The MMC model is still too complicated to be able to predict the universality class it belongs to. In fact, it is not even possible to anticipate its qualitative dynamics: the fact it produces coarsening is not trivial at all. Once noticed that simulations do show coarsening, it is natural to expect an exponent n strictly smaller than $\frac{1}{2}$, because conservation laws always slow down coarsening. In fact, we will find $n = \frac{1}{3}$, a very common value for systems where the order parameter is conserved. However, our model has two conserved quantities and cannot be mapped to any known model. Therefore, this is not a standard result. Rather, it highlights certain properties which might be common to more complicated systems.

The paper is organized as follows. In section 2, we introduce the model and show some general properties of its evolution, when the initial condition is chosen within the negative temperature region. In section 3 we illustrate the coarsening process for generic initial conditions, with particular reference to the scaling behavior of the number of surviving breathers. The following two sections are devoted to a discussion of two regimes: the fast relaxation which drives the background towards an infinite-temperature state (section 4), the slow relaxation that is responsible for the coarsening process (section 5). Such studies help to identify the reason for the increasing slowness of the coarsening, that is then better clarified in section 6, thanks to an analogy with a suitable exclusion process. By combining the various elements, a justification for the exponent $n = 1/3$ is given. Finally, in section 7, we summarize the main results and mention the still open problems.

2 The model

In this section we define the model and discuss some general properties of its dynamical behavior. A positive amplitude a_i is defined on each site of a lattice of length L , where periodic boundary conditions are assumed. Two quantities are conserved during the evolution, namely the amplitude (mass)

$$A = \sum_i a_i, \quad (1)$$

and the energy

$$H = \sum_i a_i^2; \quad (2)$$

which correspond to norm and energy in the DNLS equation in the large norm-density limit [8]. The MMC model is defined as follows. Given a generic configuration at time t , a triplet $(i-1, i, i+1)$ of consecutive sites is randomly selected and updated so as to ensure that the mass and energy are locally (and thereby globally) conserved,

$$a_{i-1}(t+1) + a_i(t+1) + a_{i+1}(t+1) = a_{i-1}(t) + a_i(t) + a_{i+1}(t) \quad (3a)$$

$$a_{i-1}^2(t+1) + a_i^2(t+1) + a_{i+1}^2(t+1) = a_{i-1}^2(t) + a_i^2(t) + a_{i+1}^2(t). \quad (3b)$$

These two laws are basically equivalent to the conservation of momentum and energy in a chain of oscillators (once a_i is interpreted as the oscillator velocity) and one might thus expect similar diffusion phenomena. Here, there is, however, an additional constraint: all a_i must be positive. Therefore, the legal configurations, that are located along the circle identified as the intersection between a plane and a sphere (the above two conditions), may be further confined to three separate arcs. This happens when the maximal amplitude \bar{a} (within the triplet) is sufficiently larger than the other two amplitudes (see Fig. 1). If, for simplicity, \underline{a} is the (equal) amplitude of the two other sites, it is easy to check that a “three-arcs” solution appears when $\bar{a} > 4\underline{a}$.

Whenever this is the case, the definition of the model is completed by specifying that we restrict the choice to the same arc of the initial condition.

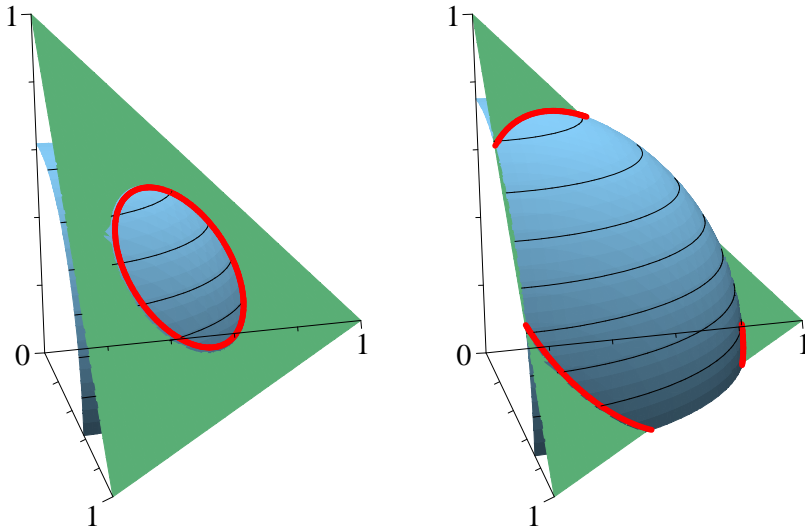


Fig. 1 Accessible MMC states (red thick line) as intersection between the plane $a_{i-1} + a_i + a_{i+1} = 1$ and a sphere with square radius 0.4 (left panel) and 0.58 (right panel).

This choice is motivated by the will to reproduce as closely as possible the original DNLS dynamics. In fact, the most important instances of three-arcs solutions are “breathers”, i.e. isolated sites with an anomalously large amplitude. Such breathers, once generated, do not appear to diffuse in the DNLS model: this property is ensured in the MMC setup by forbidding the change of arc, which would correspond to a shift of one or even two sites of the breather itself.¹

In order to identify the breathers, it is necessary to introduce an absolute threshold θ to distinguish them from the background. Depending whether $a_i > \theta$ ($a_i < \theta$) a site is classified as a breather (background) and its amplitude denoted with b_i (g_i). A typical example of the MMC evolution is shown in Fig. 2 (see the next section for a more accurate discussion, where we show also that the threshold value θ is irrelevant in so far as it is large enough).

Let us now introduce the average and the variance of the two phases as,

$$\begin{aligned} b &= \langle b_i \rangle & \sigma_b^2 &= \langle (b_i - b)^2 \rangle \\ g &= \langle g_i \rangle & \sigma_g^2 &= \langle (g_i - g)^2 \rangle \end{aligned} \quad (4)$$

where $\langle \dots \rangle$ is the spatial average, taken over all sites of the same family.

Imposing the conservation of A and H , we obtain the *exact* relations,

$$A = (L - N)g + Nb \quad (5)$$

$$H = (L - N)(g^2 + \sigma_g^2) + N(b^2 + \sigma_b^2) \quad (6)$$

¹ We have implemented two additional rules which allow for breather diffusion, but the coarsening exponent does not change (see later Fig. 4).

where N denotes the number of breathers. By defining the average amplitude and energy per site,

$$a = \frac{A}{L}, \quad h = \frac{H}{L}, \quad (7)$$

we obtain

$$a = (1 - \rho)g + b\rho \quad (8)$$

$$h = (1 - \rho)(g^2 + \sigma_g^2) + \rho(b^2 + \sigma_b^2) \quad (9)$$

where $\rho = N/L$ is the breather density (in the following, the average distance $\lambda = \rho^{-1}$ will also be used). In the limit $\rho \ll 1$,

$$g = a - b\rho \quad (10)$$

$$h = a^2 - 2ab\rho + b^2\rho + \sigma_g^2 + \sigma_b^2\rho \quad (11)$$

where we have also used the information (obtained from numerics, see next section) that $b \gg g$, because b increases in time while g saturates.

Since the entire dynamics is invariant under a change of a scale, it is convenient to rescale the amplitude to its average value a . This is perfectly equivalent to assuming that $a = 1$ (as we do from now on). As a result,

$$\rho = \frac{h - 1 - \sigma_g^2}{-2b + b^2 + \sigma_b^2}. \quad (12)$$

In [6], on the basis of purely entropic arguments, it has been found that for $h < 2$ all breathers eventually disappear, otherwise one survives (for $h > 2$), accompanied by an infinite-temperature background, characterized by a Poissonian distribution of the amplitudes. Let us see, how such predictions manifest themselves in the current setup.

From Eq. (10), for small densities, $g = 1$ and $b \simeq (h - 1 - \sigma_g^2)\sqrt{\lambda}$ (recall that now $a = 1$). Therefore, the background has a finite amplitude, while the breather amplitude scales as the square root of breather average distance. It is worth noting that $g \leq 1$ and asymptotically $g \rightarrow 1$. Therefore, for $\rho \ll 1$, since an infinite-temperature background corresponds to $\sigma_g^2 = g^2$, the request of a positive ρ in Eq. (12) corresponds to $h > 2$, the condition already derived in [6].

3 Phenomenology

In this section we illustrate the evolution, showing that it corresponds to a coarsening process. We have worked with two classes of initial conditions: (i) a fraction f of equal-height breathers sitting on a homogeneous background characterized by a uniform amplitude distribution within an interval of width δa (ICa); (ii) a homogeneous distribution of amplitudes characterized by the superposition of two exponential functions (ICb). We have verified that they give equivalent results, for the same value of h (that is systematically chosen to be larger than the critical value 2).

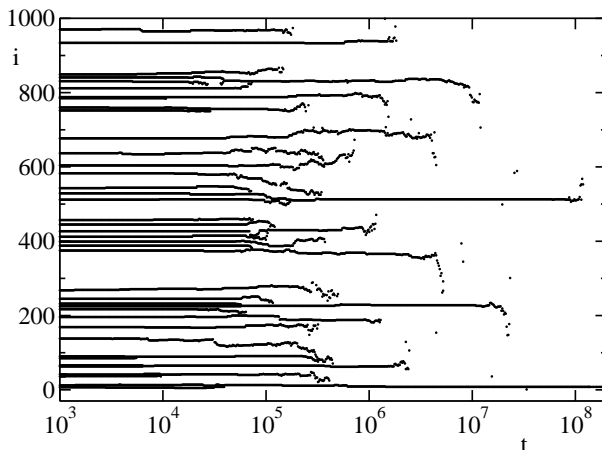


Fig. 2 Evolution of the local amplitude in a chain with $L = 1000$ and $h = 7.45$. Breathers are identified by dots and correspond to the sites i where $a_i > \theta$, with $\theta = 12.5$. The initial condition is of type ICa with parameters $f = 0.05$ and $\delta a = 0.95$.

In Fig. 2 we plot breathers positions as a function of time t , where the time is measured in numbers of Monte Carlo moves divided by the system size (L). The figure clearly shows the basic, qualitative features of dynamics: (i) breathers do not typically move, but may diffuse just before disappearing under the threshold θ (i.e. when their amplitude becomes sufficiently small) ; (ii) since the distinction breathers/background creates an artificial discontinuity, a breather may disappear and then reappear for a short time; (iii) the density of breathers decreases in time (coarsening process), because breathers gradually disappear. This process occurs when a breather goes below the threshold θ .

The first quantitative analysis of the coarsening process is done by comparing direct simulations with Eqs. (10), see Fig. 3. The constraints derived from the conservation of total energy and amplitude are found to be in good agreement with numerics even in the region of small λ . Fig. 3 clearly shows that the coarsening process (i.e. the growth of λ) is directly related to an increase of the average amplitude of the breathers, while the amplitude of the background remains finite. The same behavior occurs also for the variances σ_b^2 and σ_g^2 .

The next important quantitative aspect of dynamics concerns the coarsening law, i.e. the time dependence of the distance between breathers, $\lambda(t)$, see Fig. 4. After an initial transient, λ is found to grow in time as $\lambda(t) \sim t^n$ with a coarsening exponent $n = 1/3$ that is independent of the system size (in fact the whole curve is independent of L , if L is large). Moreover, such asymptotic behavior is largely independent of the details adopted to select a point in the available phase space. We have indeed considered two variations of the standard MMC algorithm (S). The first variant (C1) consists in selecting randomly a point either on the full circle or in the *union* of the three disconnected arcs. The second variant (C2) consists in partitioning the

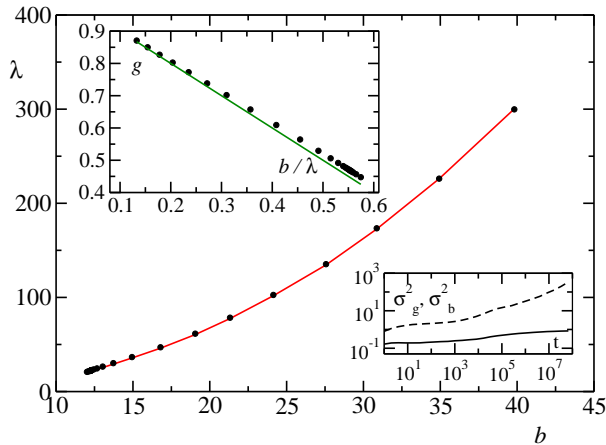


Fig. 3 Kinematics of the simplified DNLS model. Black dots refer to direct simulations of a chain of $L = 6400$ lattice sites, $h = 7.23$ and $\theta = 8.45$ (initial condition of type ICa with parameters $f = 0.05$ and $\delta a = 0.86$). The solid red line is obtained according to Eq. (12). *Upper inset*: comparison of Eq. (10) (solid green line) with simulations (black dots). Bottom-right points deviate from the expected trend as a consequence of a contribution of terms $\mathcal{O}(\lambda^{-1})$ in the early stages of coarsening. *Lower inset*: temporal evolution of the variances σ_g^2, σ_b^2 . Asymptotically σ_g^2 (black solid line) converges to a finite value corresponding to the condition of infinite temperature background, while σ_b^2 (black dashed line) increases as a consequence of the coarsening process.

circle solutions in three symmetric arcs and selecting a point of the same arc as the initial configuration (also when the full circle would be available). Altogether, the three algorithms (S, C1, C2) can be classified according to their symmetry with respect to cyclic permutations of the triplet (partial, full, absent, respectively). It is quite remarkable to notice that the scaling behavior remains unchanged even when the breathers are allowed to diffuse in real space (setup C1). This is because the coarsening does *not* proceed via coalescence (or annihilation) of the breathers: such a process is inconsistent with the simultaneous conservation of energy and mass.

Dynamics, however, allows the exchange of matter between neighboring (and next neighboring) sites. In particular, breathers exchange matter with the underlying ‘sea’, which acts as a mediator, so that breathers can effectively transfer matter between them. As a consequence of that, the breather amplitude fluctuates in time and it may go below threshold, and eventually be absorbed by the background. The key point of this evolution is the presence of a fast convergence towards local equilibrium, where the background temperature becomes infinite as shown in the next section. If two or more breathers are present, they interact via the background (section 5) which allows them to exchange matter and acquire a finite life time which is the ultimate reason for the coarsening process, that will be studied in detail in section 6.

Now let us analyze more precisely the exchange of matter between a (large) breather and the surrounding background. This study will allow to

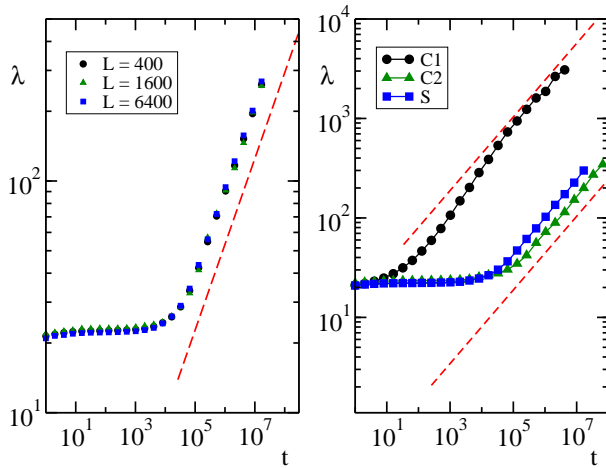


Fig. 4 *Left panel:* Average distance λ versus time t for three different system sizes $L = 400, 1600, 6400$. *Right panel:* Comparison of three different microscopic dynamics for a chain of $N = 6400$ lattice sites. Simulation parameters are the same of Fig. 3.

understand that the ‘quantum’ of transferred matter decreases with increasing breather amplitude. In order to understand the dynamics in the presence of a large breather, let us consider a triplet of consecutive sites and denote with a , ya and za , the corresponding amplitudes in decreasing order from the largest to the smallest one, so that $1 > y > z$. If $1 + y^2 + z^2 > 2(y + z + yz)$ the possible solution belongs to 3 distinct arcs. This is indeed the case when a breather is contained in the triplet since ya and za are both much smaller than a , i.e. $y, z \ll 1$. Under this assumption ($y, z \ll 1$), it can be easily shown that the rotation angle θ belongs to the interval $[-\sqrt{3}y, +\sqrt{3}z]$ and the new amplitude values are

$$\begin{aligned}
 a' &= \left[1 + \frac{\theta}{\sqrt{3}}(z - y) - \frac{\theta^2}{3} \right] a \\
 y' &= y + \frac{\theta}{\sqrt{3}}(1 - z) + \frac{\theta^2}{6} \\
 z' &= z - \frac{\theta}{\sqrt{3}}(1 - y) + \frac{\theta^2}{6}
 \end{aligned} \tag{13}$$

The largest variations are the opposite contributions $\pm\theta/\sqrt{3}$ which affect y and z , respectively. As a result, the process corresponds, to leading order, to a transfer of matter between two low-amplitude sites. This means that the breather is, in a first approximation, transparent to a propagation of matter. In order to quantify the interaction of the breather with the background, we have to consider the second order terms. Although the mass exchange is

² This expression generalizes the condition $y, z < \frac{1}{4}$ for $y = z$, mentioned below Eqs. (3).

negligible (of order $1/a$), the energy exchange is finite, no matter how big is a .

Therefore, we can conclude that it is neither the position nor the mass of the breather which performs a random motion, but rather its energy. This is preliminarily confirmed by introducing a representation, where the total energy H_i from site 1 to site i is plotted for all i versus time. The wide white regions visible in Fig. 5 record the presence of breathers, while the dark areas correspond to sequences of background sites. The dark areas coalesce, until the entire “space” is split into a single black region (the homogeneous background) and a single white region (one breather). The random fluctuations of the white areas signal the exchange of energy between neighboring breathers.

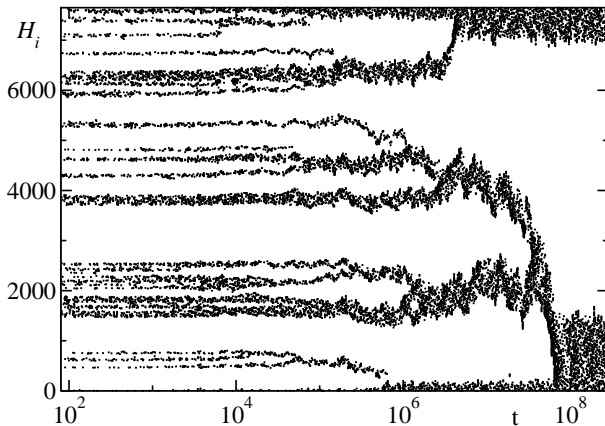


Fig. 5 Energy diffusion for a chain of 1000 sites and $h = 6.75$. The initial condition is of type ICb with exponential rates 1.725 and 0.138.

4 Fast relaxation

In this section we discuss the relaxation to equilibrium of a single breather sitting on top of a generic background. We analyze the process starting from an initial condition that is as far as possible from the asymptotic state, i.e. from the highest possible breather amplitude b , compatible with the given energy and mass densities. This condition (IC1 for later reference) is achieved by selecting a constant background (i.e. zero-temperature) with amplitude g such that $b^2 + (L - 1)g^2 = hL$ and with $(L - 1)g + b = L$. In the large L limit, $g = 1$ and $b = \sqrt{(h - 1)L}$.

As soon as the system is let free to evolve, an energy-transfer $\Delta H(t) = \langle b^2(0) - b^2(t) \rangle$ and a mass-transfer $\Delta A(t) = \langle b(0) - b(t) \rangle$ set in, which contribute to decrease the breather amplitude. Since b is and remains on the order of \sqrt{L} , the energy $\Delta H(t)$ is an extensive quantity (and one should more properly look at the intensive observable $\Delta h(t) = \Delta H(t)/L$), while $\Delta A(t)$ is subextensive, so that the density of mass in the background is

substantially unchanged. In practice, the transferred energy contributes to increase background fluctuations. Accordingly, one can equivalently monitor either $\Delta h(t)$ or the fluctuations σ_g^2 . In Fig. 6 we plot the evolution of $\Delta h(t)$ for various system sizes and fixed h . A nice data collapse is observed after introducing the scaling function

$$\Delta H = LG(t/L^2), \quad (14)$$

where $G(u) \approx \sqrt{u}$ for $u \ll 1$ and $G(u) \approx 1$ for $u \gg 1$. In practice, up until times on the order of L^2 , the energy transfer follows a diffusive law $\Delta H = \sqrt{t}$ with a diffusion coefficient that is independent of L . It is reasonable to conjecture that the energy absorption by the background is limited by the diffusion over the background itself (this question will be discussed again in a later section to justify the overall scaling behavior of the coarsening process). The diffusion stops when the background reaches the maximally entropic state, i.e. infinite temperature.

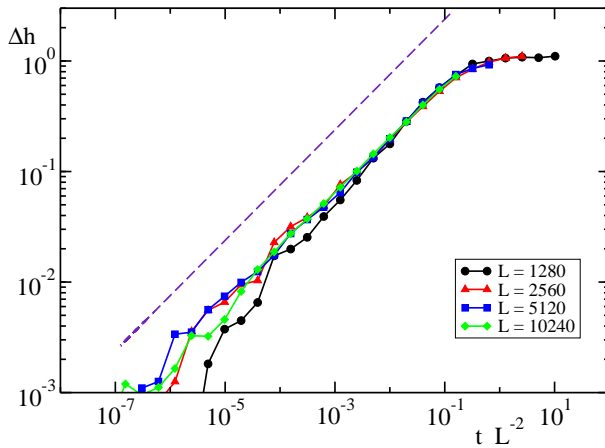


Fig. 6 Scaling properties of the energy loss $\Delta h(t)$ of a single breather relaxing on initially flat background for different system sizes L . The purple dashed line indicates a slope $1/2$. Simulations are performed selecting initial conditions of type IC1 with $b = 2\sqrt{L}$ (that corresponds to a total energy density $h = 5$).

It is convenient to approach the problem also in a different way by determining the first passage times for the rescaled breather energy $\varepsilon = b^2/L$. In practice, we fix a series of equispaced thresholds ε_j ($\delta\varepsilon = \varepsilon_{j+1} - \varepsilon_j$) and determine the first time t_j the energy crosses the j th threshold. Such times are then averaged over different realizations (see the angular brackets) to determine the effective force,

$$F_j = \frac{\delta\varepsilon}{\langle t_{j+1} - t_j \rangle}. \quad (15)$$

The results are plotted in Fig. 7 (upper panel), where the origin of the x axis is now chosen at the equilibrium value and the force is scaled by a factor

L^2 , consistently with Eq. (14). As a further check of consistency with the previous observation, notice that the force field behaves, for ε approaching the state of maximal energy ε_0 (equal to 1 for the simulations reported in Figs. 7), as

$$F(\varepsilon)L^2 \approx \frac{1}{\varepsilon_0 - \varepsilon} \quad (16)$$

which both tells us that in ε_0 there exists a barrier that cannot be overcome, and is consistent with the evolution of the breather energy. In fact, in the continuum limit a solution of the deterministic dynamical equation $\dot{\varepsilon} = F(\varepsilon)$ is

$$(\varepsilon_0 - \varepsilon) \approx \frac{\sqrt{t}}{L} \quad (17)$$

(see the dashed line in Fig. 6). Therefore, we see that the pseudo-diffusive law can be interpreted as the result of a divergence of the effective force.

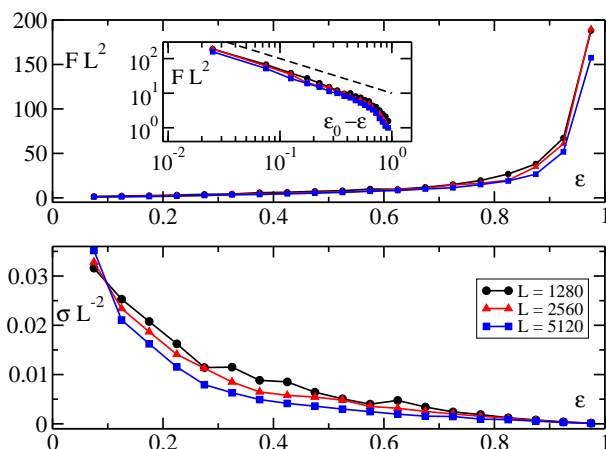


Fig. 7 *Upper panel:* Effective force $F(\varepsilon)$ calculated via first passage times for three different sizes L . The zero of the horizontal axis corresponds to the equilibrium energy. The same quantity $F(\varepsilon)$ is shown in the inset in terms of $(\varepsilon_0 - \varepsilon)$, where $\varepsilon_0 = 1$ is the initial energy. The dashed line refers to a power law $1/(\varepsilon - \varepsilon_0)$. *Lower panel:* Standard deviation of the first passage times σ . F and σ have been calculated on a sample of 100 independent initial conditions with the same parameters of Fig. 6 and $\delta\varepsilon = 0.05$.

We conclude this analysis by commenting about the amplitude of the stochastic fluctuations that are plotted in the lower panel of Fig. 7. The diffusive force σ is measured as the standard deviation of the first passage times. We see that σ vanishes for $\varepsilon = \varepsilon_0$ where fluctuations can, indeed, only decrease the breather amplitude and progressively increases until the fixed point is reached and we also see that their amplitude scales as L^2 . Altogether, this “fast” relaxation process lasts a time of order L^2 .

Notice that one could have equivalently described the scenario by monitoring the average fluctuations σ_g^2 of the background. In such a case, we would have observed that the variance of the background amplitude increases as in

a diffusion process, converging to a final state in which the interface is made of random and independent heights.

5 Slow relaxation and coarsening

In the previous section we have studied how a single breather relaxes towards the equilibrium state, where it has the optimal amplitude. In the presence of two (or more) breathers, the relaxation proceeds into two steps, see Fig. 8. First, the background converges towards the infinite-temperature state on a time scale that is analogous to that one studied in the previous section with reference to a single breather. Then, a slow random exchange of energy between the breathers starts, mediated by the background. The energy of each breather performs a random walk with the constraint that the total breather energy is approximately constant. The process proceeds until the energy of a breather becomes so low that it is adsorbed by the background, and its energy has been transferred to the other breather(s). In this section we provide a characterization of such a slow dynamics by studying a simple setup that involves only two breathers. Finally, a straightforward generalization allows to explain the coarsening exponent $n = 1/3$.

In order to cut away the transient dynamics corresponding to the relaxation of the background, the initial condition (IC2 for later reference) is now fixed by: (i) generating an infinite-temperature background, where the amplitudes a_i are i.i.d. variables, distributed according to the Poisson distribution $P(a_i) \propto \exp(-a_i/g)$ [6]; (ii) adding two equidistant breathers with amplitude $b_1, b_2 \gg g$ in a lattice of size L with periodic boundary conditions. If $L \gg 1$, the total mass is almost entirely contained in the background. Accordingly, mass conservation implies that the energy contained in the background is nearly conserved (provided that the background is at infinite temperature) and the energy contained in the two breathers conserved as well.

The first important property to point out is that the process of energy exchange between the two breathers is independent of their amplitude. More precisely, in Fig. 9 we report the probability distribution $P_2(\Delta H)$ of the energy transfer between two breathers after a time $t = 2^{19}$, with $\Delta H = [b_1^2(0) - b_1^2(t)]$. The distribution is very well fitted by a Gaussian function with zero average and appears unaffected by the choice of the initial configuration $[b_1(0), b_2(0)]$. We can therefore conclude that such a process is determined only by the properties of the stationary background in between the two breathers. From Fig. 9 it is also clear that the only relevant information concerns the time evolution of the variance $\sigma_2^2(t)$ of the distribution. According to stationarity, we can compute $\sigma_2^2(t)$ in terms of time averages, instead of averages over independent initial conditions. In formulae,

$$\sigma_2^2(t) \equiv \left\langle [b_1^2(0) - b_1^2(t)]^2 \right\rangle = \overline{[b_1^2(t+t_0) - b_1^2(t_0)]^2}, \quad (18)$$

where the overbar denotes the average over time t_0 and $\langle \dots \rangle$ denotes average over different initial conditions. Finally notice that stationarity holds as long as both breathers are present on the chain. In the following of this section we will always explore this regime.

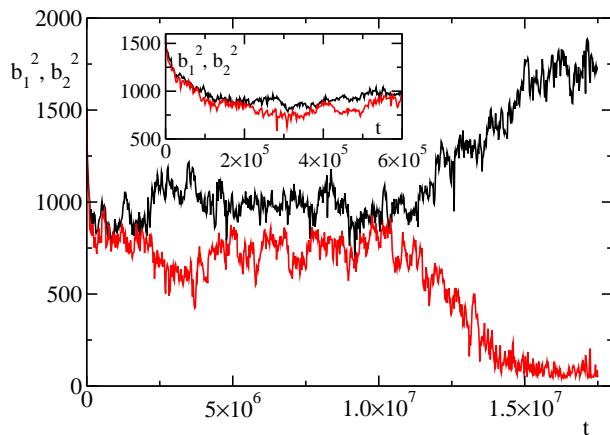


Fig. 8 Example of two breathers (with energies $b_1^2(t)$ and $b_2^2(t)$) relaxing in a chain with $L = 1280$. The initial condition is characterized by a flat background and two equidistant breathers with amplitude $b_1(0) = b_2(0) = 40$. The first part of the evolution (see the inset) corresponds to an energy transfer from both the breathers to the background. Once the background has reached the infinite temperature point (for $t \gtrsim 5 \times 10^5$), the breathers start to exchange energy among themselves until one of them is completely blown out.

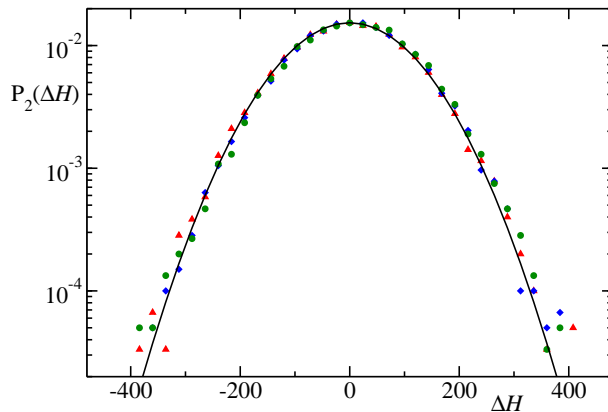


Fig. 9 Probability distribution of the energy transfer ΔH of the first breather after a time $t = 2^{19}$ in a two-breather setup with initial conditions of type IC2. Three different configurations of initial breather amplitudes have been considered: $[b_1(0) = b_2(0) = b]$ (red triangles), $[b_1(0) = b_2(0) = b\sqrt{2}]$ (blue diamonds) and $[b_1(0) = b\sqrt{2}, b_2(0) = b]$ (green circles), with $b = 100$. The black solid line refers to a Gaussian fit. Each data set is obtained from a sample of 10000 independent realizations of the MMC dynamics on a chain with $L = 640$.

In order to perform a quantitative analysis of $\sigma_2^2(t)$, we have averaged the energy fluctuations of a sample of S independent trajectories³ for different

³ The average over independent trajectories is a practical numeric tool for improving the statistics for large times t .

lattice sizes L . Upon increasing L , we keep fixed the parameters b_1, b_2 and g characterizing the initial condition IC2, so that the only change involves the distance between the two breathers.

The results reported in Fig. 10 show a growth in time of the energy fluctuations. In particular, for large enough times, $\sigma_2^2(t)$ has a linear profile, thus indicating the existence of a diffusive law. The associated diffusion constant is however inversely proportional to the system size L (and therefore also to the spatial separation of the breathers, equal to $L/2$). As a consequence, the larger the chain is, the slower the energy diffusion process is. A data collapse is finally obtained by rescaling energy and time respectively by L and L^2 .

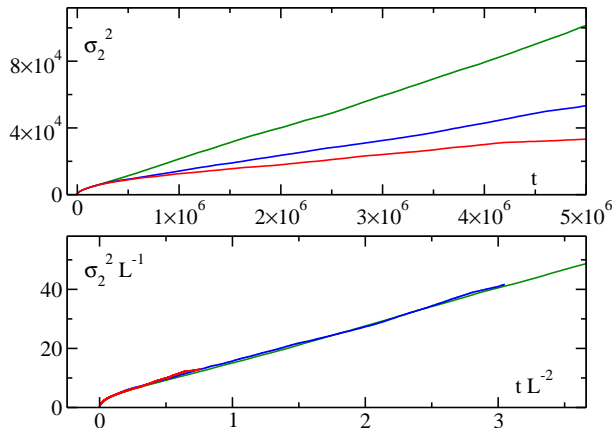


Fig. 10 *Upper panel:* Time evolution of the energy fluctuations σ_2^2 of two breathers sitting on an infinite temperature background. Lines from top to bottom refer to lattice sizes $L = 640, 1280, 2560$, respectively. Data are obtained from a set of $S = 10$ samples evolved for 3.4×10^7 time units, starting from an initial condition of type IC2 with two breathers of amplitude $b = 100$. Running averages are performed monitoring time differences from $dt = 10^3$ to $dt = 5 \times 10^6$ time units. *Lower panel:* Data collapse on the universal function $f_2(u)$ after the rescaling $t \rightarrow t/L^2 = u$ and $\sigma_2^2 \rightarrow \sigma_2^2/L$.

A more general description of the overall scenario can be obtained by comparing the results of Fig. 10 with the same kind of simulations performed with only one breather in the chain, i.e. in a equilibrium regime. Energy fluctuations, denoted with $\sigma_1^2(t)$, are now expected to be *finite* for large enough times, with the characteristic scaling $\mathcal{O}(L)$ with the system size. Fig. 11 points out the equivalence of the dynamic behavior in presence of one *and* two breathers for small times. In this regime, in fact, a breather cannot know about the existence of some other breather in the chain and behaves as if it were at equilibrium (local equilibrium). Only after a characteristic time $t_c \sim L^2$ a “bifurcation” occurs, separating the linear growth of fluctuations in presence of two breathers from the saturation required by (global) equilibrium in presence of only one breather.

The results plotted in Figs 10 and 11 can be summarized by the following scaling relations for the variances σ_1^2, σ_2^2 of the energy of a single breather

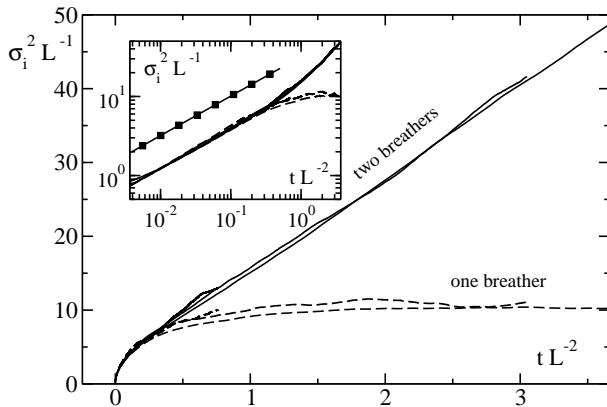


Fig. 11 Comparison of the universal functions $f_1(u)$ and $f_2(u)$ in presence of one breather (dashed lines) and two breathers (solid lines), respectively. The functions $f_i(u)$ are extracted by means of the rescaling $t \rightarrow t/L^2 = u$ and $\sigma_i^2 \rightarrow \sigma_i^2/L$ for three different sizes $L = 640, 1280, 2560$. Simulations are performed using the same parameters specified for Fig. 10. The inset shows the behavior of $f_i(u)$ for small u . The square-solid line is a power law with exponent $1/2$.

when the system is made up of one and two breathers, respectively:

$$\sigma_i^2 = L f_i \left(\frac{t}{L^2} \right) \quad (19)$$

where $f_1(u) \approx f_2(u) \approx \sqrt{u}$ for $u \ll 1$, while at large $u \gg 1$, $f_1(u) \approx 1$ and $f_2(u) \approx u$. In particular, $\sigma_2^2 \approx t/L$ at large times, which gives a first explanation of the coarsening exponent $n = 1/3$. In fact, during the coarsening process the energy of the breather scales as L , where L is now the distance between breathers. Therefore, the time to allow a breather to disappear corresponds to $\sigma_2^2 \sim L^2$, i.e. $t/L \sim L^2$, and finally $L \sim t^{1/3}$.

6 Comparison with a Partial Exclusion Process (PEP)

In the previous sections we have provided a characterization of the simplified DNLS stochastic model in the presence of localized excitations. The very existence of such localized states has been related to the simultaneous conservation of energy and mass. If, for example, we suppressed one conservation law, we would recover a standard diffusion process, always relaxing to an homogeneous state, with no room for breathers. On the other hand, the stochastic process generated by the MMC rule turns out to be nontrivial even at a microscopic level, since the available phase space depends nonlinearly on the local amplitudes. From a macroscopic point of view, this property leads to a nonlinear Fokker-Planck equation. The question is therefore whether it is possible to further simplify the DNLS model, keeping all the essential features of its dynamics. This possibility might allow to obtain a more rigorous explanation of the coarsening exponent $n = 1/3$.

In this section we show that a simple partial exclusive process (PEP) can reproduce the coarsening observed in the DNLS context. The continuous variable a_i is replaced by a discrete, integer amplitude h_i which represents the number of particles on site i . The evolution rule is purely stochastic: once an ordered pair of neighbouring sites (i, j) ($j = i \pm 1$) has been randomly selected, the transformation $(h_i, h_j) \rightarrow (h_i - 1, h_j + 1)$ is made if and only if $h_i > 0$ and $h_j \neq 1$. In practice, one can divide the lattice into two parts: (i) breather-sites ($h_i > 1$) which can freely exchange particles with the surrounding environment; (ii) background ($h_i = 0, 1$) which behaves as in a standard exclusion process. As soon as any given height h_i decreases down to 1, the breather is irreversibly absorbed by the background. Therefore, we can expect this model to exhibit a coarsening dynamics, which will be compared to the dynamics of the simplified DNLS model.

In the previous sections it proved useful to study the relaxation of two-breather states towards a final configuration characterized by a single breather. We are now going to do the same for the PEP model: see Fig. 12, where a configuration with with breathers is sketched.

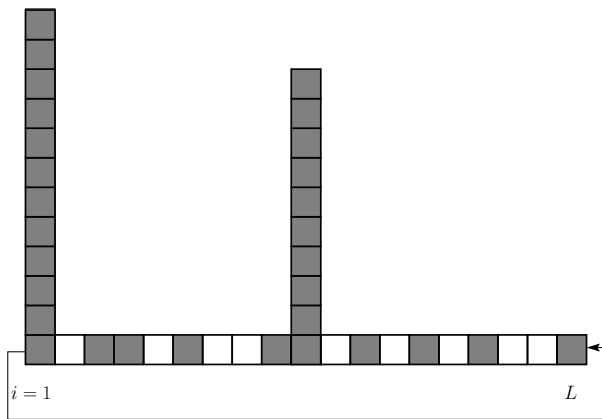


Fig. 12 The simplified model: two columns of bricks (grey squares) interact exchanging particles through a channel modeled by a partial exclusion process (PEP) with periodic boundary conditions. Each site of the channel can sustain no more than one particle at a time. Particles evolve according to a standard diffusion algorithm endowed with the exclusion rule.

We start by investigating the transport properties of the background field in both models with the help of the power spectrum of the long-wavelength Fourier modes. In order to study qualitatively similar dynamic regimes, we have chosen two initial conditions with the same density of particles, in a condition of maximum entropy, i.e. infinite temperature. In the MMC model, this requirement amounts to a Poissonian initial distribution of the amplitudes [6] with average g , while for the PEP model the same regime corresponds to an average occupation number $\tilde{\rho} = 0.5$. Accordingly, we have chosen $g = \tilde{\rho} = 0.5$. The results are plotted in Fig. 13: as expected the power spectrum of the PEP model is well fitted by a Lorentzian distribution, a clear evidence of diffu-

sion. A diffusive behavior in the MMC model is not so straightforward, as its microscopic rule is much more complicated than a standard diffusion algorithm, but this is what we find also in this case. Moreover, the power spectra of the two models nicely overlap in a wide region of the Fourier space and prove the validity of the PEP model as an effective reduction of the MMC algorithm. On the other hand, the slight gap in the low frequency region suggests a different behavior of the (static) diffusion constants associated to the two dynamics.

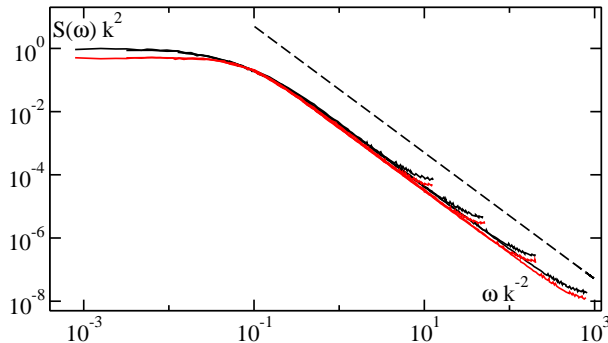


Fig. 13 Power spectra $S(\omega)k^2$ versus ωk^{-2} of the MMC dynamics (black solid line) and the PEP model (red solid line) for low- k Fourier modes, with $k = 2\pi m/L$ and $m = \{1, 2, 4, 8\}$. Data refer to MMC (PEP) chains with length $L = 256$ in an infinite temperature state with average occupation number $g = 0.5$ ($\bar{\rho} = 0.5$). The black dashed line is a power law with exponent -2 .

Having ascertained that perturbations propagate across the background diffusively in both models, we analyze the dynamics in the presence of breathers. In the PEP model, we proceed by determining the mean lifetime τ of a couple of columns separated by two channels of length $L/2$ (L being the total size of the system). The quantity τ is defined as the average time that is necessary for one of the two columns to be destroyed (i.e. to reach a unitary height), supposing that the columns have initial heights $h_0 = kL$, where k is a positive constant. Fig. 14 clearly shows that τ scales with the system size as a power law, $\tau \sim L^3$. This scaling law is the same as for the original MMC model and it is responsible for the characteristic coarsening process of the breathers with an exponent $n = 1/3$.

Let us now evaluate the coarsening time for the PEP model and compare it with numerical results shown in Fig. 14. If $h_0 = kL$ is the initial breather height, the typical time τ for the disappearance of one breather is given by the relation $h_0^2 = \tau/\Delta t$, where Δt is the typical time for exchanging one particle between the two breathers. If the system were composed by the two neighboring breathers only, $\Delta t = 1$, but in our case, once the “emitting” breather has been chosen, the exchange becomes effective only if the move (breather) \rightarrow (neighbouring site) is allowed and if the diffused particle reaches the other breather before being re-absorbed by the emitting breather. The move (breather) \rightarrow (neighbouring site) occurs with probability

1/2, which is the average occupancy of background sites. The diffusion to the other breather occurs with probability $2/L$ [13], where $L/2$ is the distance between breathers. Therefore $\Delta t = L$ and

$$(kL)^2 = \frac{\tau}{L} \quad (20)$$

so that

$$\tau = k^2 L^3 \quad (21)$$

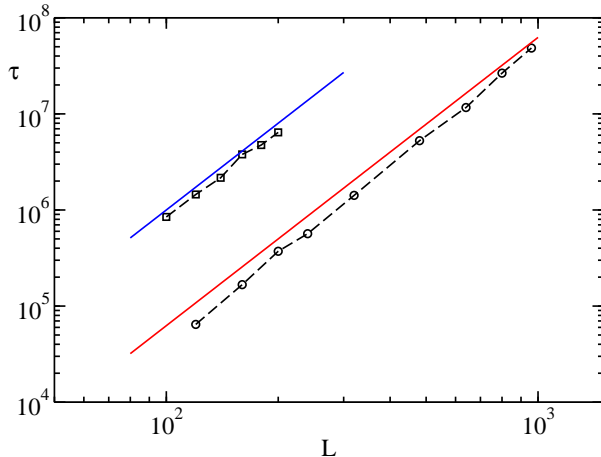


Fig. 14 Average lifetime τ of a couple of columns exchanging particles through a PEP channel with length $L/2$. The columns have equal initial height h_0 linearly increasing with the system size L as $h_0 = kL$. Simulations have been performed choosing $k = 1$ (open squares) and $k = 1/4$ (open circles). The initial configuration of the channel corresponds to an infinite temperature state with average occupation number $\bar{\rho} = 0.5$. Solid lines are defined by the equation $\tau = k^2 L^3$ with $k = 1$ for the upper blue line and $k = 1/4$ for the lower red one.

7 Summary and conclusions

In this paper we have thoroughly studied a microcanonical Monte Carlo model which approximately reproduces the evolution of a DNLS equation for large mass densities ($a \gg 1$). In the so-called negative temperature region (which corresponds to an energy density $h > 2a^2$), the spontaneous formation of breathers is observed (see Figs. 2 and 5).

Our studies reveal that, in agreement with the entropic arguments put forward in Ref. [5], the system converges towards a stationary state composed of a single breather in equilibrium with an infinite temperature background. The evolution is characterized by two time scales. Over “fast” times (on the order L^2), the background equilibrates at infinite temperature, while a population of breathers forms to store the “excess” energy that cannot be

contained in the background. This phenomenon can be attributed to the existence of two positive-defined conserved quantities (energy and mass) which scale with a different power of the local variable (quadratic and linear, respectively): as a result, breathers can contain extensive amounts of energy, while marginally contributing to the mass which is, instead, essentially stored in the background. This regime has been first investigated in the simplest possible setup: a single breather sitting on a flat background. The data in Figs. 6 and 7 clearly show the presence of a time scale L^2 .

On a longer time scale L^3 , the evolution is characterized by a coarsening process, characterized by an exchange of energy among the breathers, until they progressively disappear, leaving just one alive. Coarsening occurs on a purely stochastic basis, because a breather may lose some of its energy, which diffuses along the background possibly reaching a neighboring breather. Accordingly, the breather height fluctuates and, when a breather goes below threshold, it is “adsorbed” by the infinite temperature background and it cannot appear again. The coarsening exponent $n = \frac{1}{3}$ (see Fig. 4) is a consequence of three facts. First, conservation of mass and energy implies that the breather energy (not breather height, i.e. mass) performs a random walk. Second, conservation of mass and energy implies that the energy of a breather scales as the distance λ between breathers. Third and finally, the elementary time scale for exchanging mass between breathers is set by the inverse of the probability that a “quantum” of mass released by a breather is able to attain the neighboring breather instead of going back. This probability scales as $1/\lambda$.

In order to give a more firm basis to the derivation of $n = \frac{1}{3}$, the furtherly simplified PEP model has been introduced and analysed. Such a model shows remarkable similarities with the original DNLS dynamics: (i) the condensation onto a single site appears above a critical value (defined by the mass density $\tilde{\rho} = 0.5$ in the PEP model and by the energy density $h = 2$ in the simplified DNLS); the same scaling exponent is found in the two models. It is, however, necessary to recall a crucial difference: the presence of two rather than just a single conservation law in the simplified DNLS model. The very same difference exists with other models where a similar scenario can be found: the Kinetic Ising Model with conserved magnetization [14] and a class of zero-range processes [15].

Finally, going back to the original DNLS model, it is worth recalling two major simplifications introduced in this paper: (i) the interaction energy between neighbouring sites has been neglected (the MMC model indeed corresponds to the high mass-density limit of the DNLS equation); (ii) dynamical effects are disregarded (the model is purely stochastic). The first limitation could be removed by reintroducing the interaction term in the original Hamiltonian. As a result, one would be, however, forced to account also for the phase dynamics (absent in the MMC model) with the related difficulty (impossibility) of deriving explicit microcanonical transformations. This is, nevertheless, a route that would be worth to explore, especially to check the robustness of the coarsening process herein investigated.

As for possible dynamical effects, one cannot exclude that the dynamical arrest of the coarsening observed in [8] is partly due to the weak coupling of

the rapidly rotating breathers with the background which makes energy and mass exchanges even slower than in our stochastic process.

References

1. P.G. Kevrekidis, The Discrete Nonlinear Schrödinger Equation (Springer Verlag, Berlin, 2009)
2. S. Flach, A.V. Gorbach, *Physics Reports* **467**(1), 1 (2008)
3. K. Rasmussen, T. Cretegny, P. Kevrekidis, N. Grønbech-Jensen, *Phys. Rev. Lett.* **84**(17), 3740 (2000)
4. B. Rumpf, *Phys. Rev. E* **69**, 016618 (2004)
5. B. Rumpf, *EPL (Europhysics Letters)* **78**(2), 26001 (2007)
6. B. Rumpf, *Physical Review E* **77**(3), 036606 (2008)
7. B. Rumpf, *Physica D: Nonlinear Phenomena* **238**(20), 2067 (2009)
8. S. Iubini, R. Franzosi, R. Livi, G.L. Oppo, A. Politi, *New Journal of Physics* **15**(2), 023032 (2013)
9. A.J. Bray, *Advances in Physics* **51**(2), 481 (2002)
10. P. Politi, C. Misbah, *Phys. Rev. E* **73**, 036133 (2006)
11. P.C. Hohenberg, B.I. Halperin, *Rev. Mod. Phys.* **49**, 435 (1977)
12. M.R. Evans, T. Hanney, *Journal of Physics A: Mathematical and General* **38**(19), R195 (2005)
13. S. Redner, A guide to first-passage processes (Cambridge University Press, 2001)
14. S.J. Cornell, K. Kaski, R.B. Stinchcombe, *Phys. Rev. B* **44**, 12263 (1991)
15. C. Godrèche, *Journal of Physics A: Mathematical and General* **36**(23), 6313 (2003)